RSC Advances

ROYAL SOCIETY OF CHEMISTRY

www.rsc.org/advances

Journal Name

ARTICLE

Synthesis and characterization of cyclic 9,9-bis(4-hydroxyphenyl)fluorine (phenylene phosphonate) oligomer and its flame retardancy application

Received 00th January 20xx,
Accepted 00th January 20xx

DOI: 10.1039/x0xx00000x

www.rsc.org/

Nana Li [a,b], Guowei Jiang [a], Guangyuan Zhou *[,a]

A novel solid flame retardant cyclic 9,9-bis(4-hydroxyphenyl)fluorine (phenylene phosphonate) (CPFP) oligomer was synthesized in high yields by the reaction of phenylphosphonic dichloride with 9,9-bis(4-hydroxyphenyl)fluorine under pseudo-high-dilution conditions via polycondensation. Detailed structural characterizations of this oligomer were conducted by matrix-assisted laser desorption/ionization time-of-flight mass spectrometry (MALDI-TOF-MS), ^{1}HNMR, ^{31}PNMR and FTIR. Furthermore, the flame-retardant efficiency of this oligomer in polybutylene terephthalate (PBT) was studied using limiting oxygen index (LOI) and UL-94 tests. After the addition of CPFP, the LOI increased and the UL94 V-0 rating was achieved. The occurrence of an interaction between CPFP and PBT was elucidated by thermogravimetric analysis (TGA), FTIR and pyrolysis/GC/MS. Results showed that the CPFP oligomer could change the degradation path of PBT and improves the char formation of the PBT/CPFP system. The residual morphologies of residues of the PBT/CPFP25% system were investigated by scanning electron microscopy (SEM). SEM investigations revealed that the residual chars contained polyphosphoric or phosphoric acid, which plays an important role in the process of carbonization.

Introduction

At present, for the development of flame retardants, the following conditions should be satisfied: flame retardant with high efficiency, good thermal stability, good compatibility with polymer, no adverse effect on the mechanical properties of polymer materials, such as electronic, weather resistance, non-toxic, pollution-free, etc. Although halogen-containing flame retardants have been widely used, these substances cannot meet environmental requirements. Thus, the discovery of environmentally friendly phosphorus-containing flame retardants has become an important research topic.[1-3] Organic phosphorus-containing flame retardants have both fire retardation and plasticizing effect. To date, linear polymeric flame retardants have been successfully used as flame retardants in polymeric material.[4-12] Aromatic phosphates, such as resorcinol bis(diphenyl phosphate) (RDP), poly(sulfonyldiphenylene phenylphosphonate) (PSPPP) and bisphenol A bis(diphenyl phosphate) (BDP) are effective in polymers which produce phenolic functionalities upon pyrolysis, for example in bisphenol A poly-carbonate (PC) and PBT.[13-17] Cyclic oligomers offer a unique combination of low melt viscosity and the possibility of undergoing controlled polymerization in the melt without the liberation of volatile byproducts, which makes them good candidates in advanced thermoplastic compositions.[18, 19] Also, cyclic oligomers can be well dispersed in polymer matrix and offer a good compatibility with polymer materials. In addition, phosphorus-containing cyclic oligomers have good flame retardant effect on polymeric material.

In the current research, we introduce cyclic 9,9-bis(4-hydroxyphenyl)fluorine (phenylene phosphonate) oligomer, aiming at the cyclization reaction of phenylphosphonic dichloride (PPD) with 9,9-bis(4-hydroxyphenyl)fluorine to develop a novel cyclic oligomer under pseudo-high-dilution conditions. The synthesis scheme of cyclic (arylene phosphonate) oligomer is shown in Fig. 1. The Synthesis conditions are mild and convenient. Notably, cyclic 9,9-bis(4-hydroxyphenyl)fluorine (phenylene phosphonate) oligomer was used as additive agent based on the flame-retardant property. And we chose PBT as the matrix resin for studying the flame retardant effect of cyclic (arylene phosphonate) oligomer. We have tested the use of the cyclic (arylene phosphonate) oligomer and its combination as flame-retardant additive in PBT.

Experimental

Synthetic procedures

Cyclic oligomer CPFP was synthesized in a 2 L four-neck round-bottom flask equipped with nitrogen inlet, thermometer, injection port and stirrer. The flask was charged with 200 mL of dichloromethane and 2 ml of triethylamine at 0 °C. 7 mmol 9,9-bis(4-hydroxyphenyl)fluorine and equimolar PPD were dissolved in

[a] Key Laboratory of Polymer Ecomaterials, Changchun Institute of Applied Chemistry, Chinese Academy of Sciences, Changchun, Jilin, 130022, China.
[b] University of Chinese Academy of Sciences, Beijing, 100049, China.
Electronic Supplementary Information (ESI) available: [details of any supplementary information available should be included here]. See DOI: 10.1039/x0xx00000x

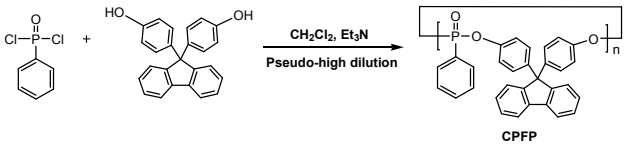

Fig. 1 Synthesis scheme of cylic 9,9-bis(4-hydroxyphenyl)fluorine (phenylene phosphonate) oligomer.

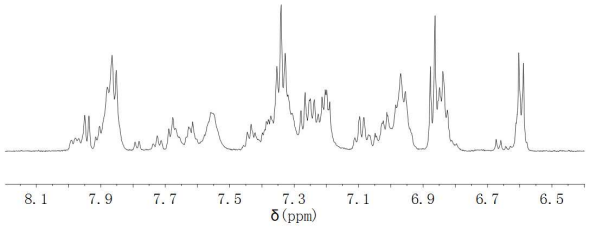

Fig. 2 ^{1}H NMR spectra of CPFP oligomer.

250 mL dichloromethane, separately. The two kinds of solution were added dropwise to the mixture by peristaltic pump in the mechanically stirred flask in an equimolar fashion over a period of 8 h. After the addition, the mixture was stirred for another 2 h. The solvent was then removed from the filtrate at reduced pressure. The residue was boiled in distilled water for thrice. The desired cyclic oligomer were obtained as a pale white powder and dried in a vacuum oven (80 °C) for 12 h. The yield of CPFP was 2.73g (yield: 82%). FTIR (KBr, cm^{-1}): 1133, 1271, 1170 (P=O), 1200 and 1017 (P-O-C) cm^{-1}. ^{1}H NMR (DMSO-d_6, ppm): δ6.62 (d, 4H), 6.88(m, 4H), 7.28(m, 2H), 7.36(m, 4H), 7.58(m, 2H), 7.69(m, 1H), 7.88(m, 2H), 7.97(d, 2H) ppm (Fig. 2). ^{31}P NMR (DMSO-d_6, ppm): 11.59(d, 1P).

Materials and methods

Phenylphosphonic dichloride, 9,9-bis(4-hydroxyphenyl)fluorine were purchased from Alfa and used as received. PBT (PBT1084, density 1.31±0.02 g/cm^3, intrinsic viscosity 0.84±0.02 cm^3/g) used in this study was obtained as pellets from Nantong Xingchen Synthetic Material Co. Ltd., China. PBT pellets were dried for 24 h in a vacuum oven at 120 °C before use, whereas other reagents and solvents were obtained commercially and used without further purification.

Matrix-assisted laser desorption/ionization-time of flight mass spectra (MALDI-TOF-MS) were recorded on a LDI-1700 instrument at a wavelength of 337 nm (N_2 laser light) using 1, 8, 9-dithranol as the matrix. The instrument was operated in a positive linear mode. NMR proton spectra were recorded on a Varian Unity-400 NMR spectrometer at 400 MHz in DMSO-d_6 using tetramethylsilane (TMS) as the standard. Thermal gravimetry analysis (TGA) was performed with a Mettler Toledo TGA851 thermal gravimetric analyzer using a continuous nitrogen flow (50 ml/min) and a heating rate of 10 °C/min from 30 to 700 °C. The sample was approximately 10-20 mg. Different scanning calorimetry (DSC) was carried out on a Mettler Toledo DSC1 Stare under continuous nitrogen flow (200 ml/min). The samples were first heated from 25 to 250 °C at a rate of 10 °C/min to remove thermal history, and cooled at a rate of 10 °C/min 25 °C, and then reheated to 250 °C at a rate of 10 °C/min, to obtain the melting temperature (T_m) and crystallization temperature (T_c).The chemical structures of combustion residue were characterized using a VERTEX 70 FTIR (Bruker Optics) spectroscope in KBr pellets. It was collected in the region of 4000-400 cm^{-1} with a spectral resolution of 2 cm^{-1} and 64 scans. The residues of infrared study were obtained after thermal treatment by TGA equipment. Field emission scanning electron microscope (FESEM, XL30 ESEM FEG) was used for the observation of morphology. First the sample was heated in a temperature-programmable microfurnace pyrolyser (CDS5000-1500) under continuous helium flow (1 ml/min). The gas thermal degradation products were identified by GC/MS (Agilent 5975). In gas chromatogram, a HB-1 nonpolar column was temperature-programmed from 80 °C (3 min) to 280 °C (20 min) at a heating rate of 10 °C /min. For the MS measurement, ionization was carried out by electron impact (EI) at 70 eV, and a mass range between 20 and 600 amu was scanned at a rate of 2 s/scan. Mass spectrometric identification was carried out using NIST2008 standard spectral library. In the few cases, when compounds were not included in the libraries, they were identified on the basis of both the molecular ion *m/z* value and of the ion decomposition pattern constructed for the best fit with the mass spectrum.

Preparation of composites

PBT pellets with different contents of CPFP (15 wt.%, 20 wt.%, and 25 wt.%) were mixed. Subsequently, melt blends were performed using a Haake Rheocord 90 internal mixer at 230 °C for 5 min with a rotation speed of 60 rpm. Samples were then molded by compression for the standard test. The neat PBT used as a standard was treated in the same manner. All blends included 1 wt.% of Polytetrafluorethylene (PTFE).

Combustion test

The combustion performance was studied by the limited oxygen index (LOI) test and the vertical burning ratings (UL-94) test standard on 3.0 mm specimens in the vertical configuration. LOI was measured using an LOI instrument (HC-2 Analytical Instrument Factory, China) on sheets (130*6.5*3 mm) according to the standard oxygen index test (GB2406-82, China). The test was based on the determination of the percentage of oxygen in a gas mixture (O_2 and N_2), which will just sustain the burning of 50 mm length of a sample for 180 s. According to the UL-94 test, the sample rod (130*13.0*3.0 mm) was placed in a holder in a vertical position and the lower end of the rod is contacted by a flame for 10 s thus initiating burning.

Results and discussion

Characterization of oligomer CPFP

The cyclic nature of the oligomer was confirmed by matrix-assisted laser desorption/ionization-time of flight mass

spectrometry (MALDI-TOF-MS). A relatively clean positive spectrum with reasonable signal-to-noise ratio was obtained. MALDI-TOF-MS indicated that the oligomer CPFP consisted principally of macrocycles with repeating units of 2 to 7. Fig. 3 shows six strong peaks, and the peak-to-peak mass increment was 472.5. These signals were caused by the molecular ion peaks for $[Mn+H]^+$. The MALDI-TOF-MS spectrum revealed cyclic oligomers from dimer (n = 2, m/z = 945.9) up to heptamer (n = 7, m/z = 3308.2). Traces of linear oligomers were also present, and the peaks can be caused by the protonated $(AB)_n$ (n = 3 to 5).

According to the Jacoson-Stockmayer Theory,[20] the component distribution of cyclic oligomers follows the formula:

$$c_n = Bn^{-\gamma}\chi^n$$

Where c_n is the concentration of cyclic oligomers with polymerization degree of n. B is a constant which is related to reactants and solvent. The χ is the rate of reacted terminal group. When the reaction degree is large, χ closes to 1. The process of reaction is under a pseudo-high dilution condition, and the concentration of reactive monomers in the reaction system is very low ($<10^{-4}$mol/L). At this time, the composition distribution of oligomers affected by the center bond angle of the bisphenol monomer. The value of γ increases with the center bond angle of the bisphenol monomer increasing. When the center bond angle is around 109°, there is a surge phenomenon. The larger the value of γ is, the bigger the concentration of small ring compound is.[21] In addition, the movement of molecular chain is not good for formation of big ring compound.

Flammability properties

The LOI value and the UL-94 test results are the two parameters used to evaluate the flammability of flame-retardant materials. The LOI and UL-94 sample results are presented in Table 1. Notably, the addition of CPFP was beneficial to improve the flame retardancy of PBT. The LOI value increased to 28.4% when the amount of CPFP was 20%. Given the UL-94 test results, the sample can reach the UL-94 V-0 rating when the content of CPFP was 20%. Although the addition of CPFP cannot eliminate the melt dripping of PBT, the dripping of blends without flame cannot ignite the cotton during the test compared with the pure PBT. Thus, this dripping can reduce the loss from burning caused by dripping.

Thermal stability analysis

The effect of the fire retardants (CPFP) on the thermal property of PBT was studied by DSC. Fig. 4 present the DSC heating thermogram curves of neat PBT and PBT/CPFP25%. On heating, multiple melting peaks were observed in the two samples. Adding CPFP led to the decrease of all the melting temperatures. For pure PBT T_{m1} and T_{m2} were 217.4 °C and 225.2 °C, but for PBT/CPFP25% mixture the T_{m1} and T_{m2} were 211.3 °C and 221.4 °C.

Fig. 5 shows the thermogravimetric curves of PBT, CPFP and PBT/CPFP25% mixture (experimental and calculated) under nitrogen atmosphere. The thermogravimetric data of PBT, CPFP and their mixture are summarized in Table 2. The temperature at which the weight loss exhibits 5 wt.% is defined as the onset decomposition temperature (T_{onset}). The temperature at which the degradation rate reaches a maximum is defined as T_{max}. As shown in Table 2, the thermal degradation of pure CPFP starting at 327.8 °C was a two-step decomposition, and a large amount of charred residue (47.8%) was left at 700 °C in nitrogen atmosphere. By contrast, the thermal degradation of pure PBT, which was also a two-step decomposition, started at 372.3 °C and showed no residue under the same condition. The T_{onset} of PBT/CPFP composites at the first step were slightly lower than that of pure PBT, and the onset decomposition temperature decreased as the amount of CPFP increased.

Fig. 5 indicates that the addition of CPFP improved the char formation of PBT. There is finally about 17.4% of solid residue at700 °C in inert atmosphere. Thermogravimetry provides evidence that CPFP interacted with PBT upon pyrolysis because of the increase in solid residue and the decrease of the onset decomposition temperature of the formulation containing CPFP. This is well demonstrated by comparing experimental and

Table 1 LOI (%) values and UL-94 of different PBT samples

Samples	Ignition the cotton	Observed dripping	LOI (%)	UL-94
PBT	Yes	drip	20.2	-
PBT/CPFP15%	Yes	drip	24.8	V-2
PBT/CPFP20%	No	drip	28.4	V-0
PBT/CPFP25%	No	drip	30.2	V-0

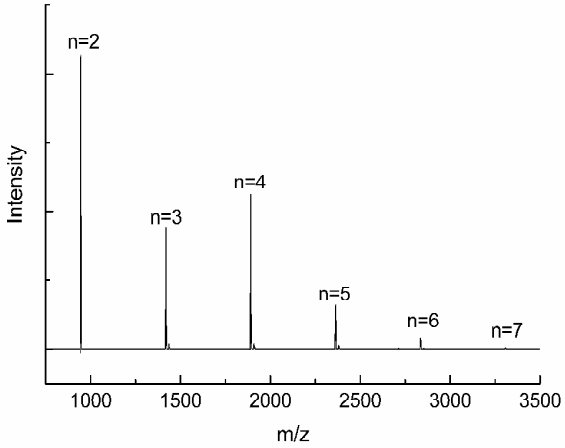

Fig. 3 MALDI-TOF-MS spectrum of CPFP oligomer.

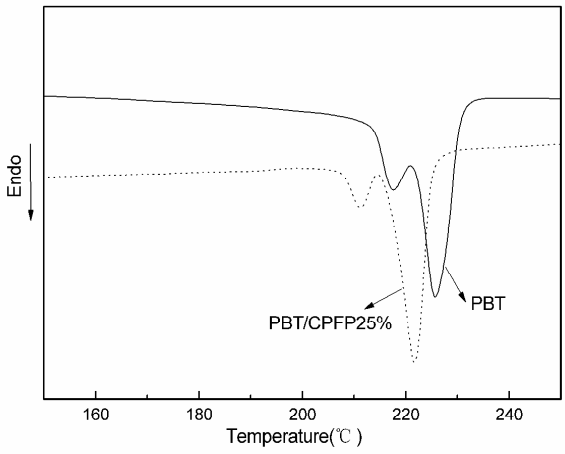

Fig. 4 DSC thermograms recorded during the heating step (10 °C/min, N_2) for PBT and PBT/CPFP25%.

Journal Name

ARTICLE

Table 2 Thermal property of different samples in nitrogen.

Sample	T_{onset} (°C)	T_{max} and weight loss at this stage				Char yield/% (700°C) (by experimental)	Char yield/% (700°C) (by calculated)
		$T_{max,1}$ (°C)	Weight loss (%)	$T_{max,2}$ (°C)	Weight loss (%)		
CPFP	327.8	366.3	11.2	567.3	44.9	47.8	
PBT	372.3	403.3	51	469.3	93.6	0	-
PBT/CPFP15%	366.8	399	65.1	474.1	86.7	8.6	5.79
PBT/CPFP20%	361.8	391.7	53.8	455.5	81.5	11.7	8.24
PBT/CPFP25%	353.5	380.4	50	473.2	77.2	17.4	10.7

T_{onset} is the onset decomposition temperature at which the weight loss is 5%.
T_{max} is the maximum-rate degradation temperature.
$T_{max,1}$ is the maximum-rate degradation temperature of first stage.
$T_{max,2}$ is the maximum-rate degradation temperature of second stage.

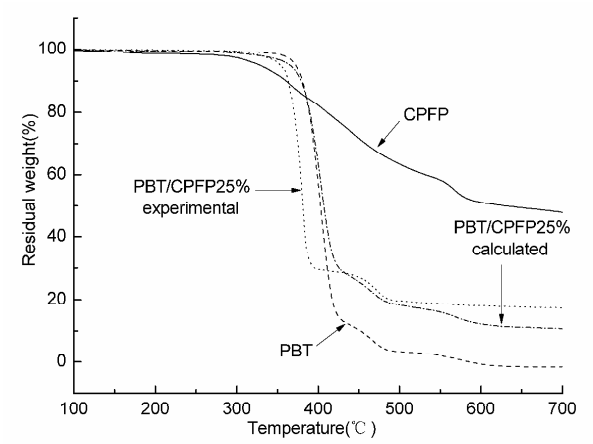

Fig. 5 Thermogravimetry of PBT, CPFP and PBT/CPFP25% mixture (experimental and calculated).

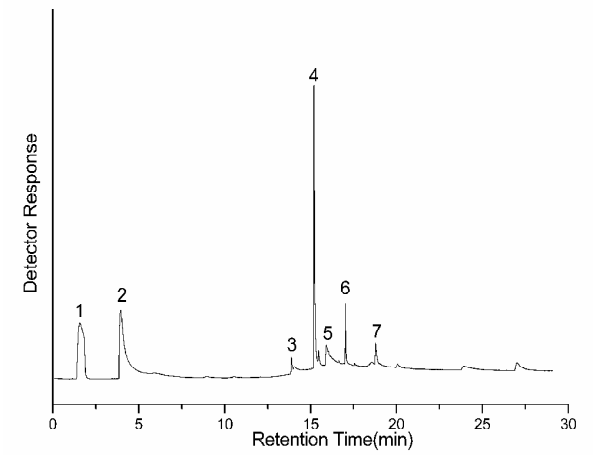

Fig. 6 Gas chromatogram of the gaseous pyrolysis products of CPFP obtained on heating at 600 °C (50 °C/min) for 1 min, for peak assignment see Table 3.

calculated thermograms (Fig. 5). The calculated curve is a linear combination of the thermograms of the single components of the mixture, therefore it is representative of a non-interacting behavior. At the end of the first step, weight loss was lower than that of pure PBT, and CPFP restrained the decomposition of PBT. This result also shows that CPFP is a good char former: the amount of solid residue obtained at 700 °C increased more than 40 percent as much as expected from their independent thermal decomposition behavior. The similar effect was observed in papers before.[22-26]

Pyrolysis/GC/MS study

In order to discuss more detailed degradation processes on the basis of the chemical information about the gaseous pyrolysis products, pyrolysis/GC/MS measurement was carried out. CPFP, PBT and PBT/CPFP25% were pyrolysed at 600 °C by pyrolysis/GC/MS to get a more precise insight into the products of thermal decomposition. According to the NIST2008 standard spectral library, we inferred the structures of the products. Table 3 shows the main pyrolysis products of CPFP from the

Table 3 The pyrolysis products of CPFP at 600 °C

Peak No.	Molecular mass (*m/z*)	Compound
1	78	
2	94	
3	242	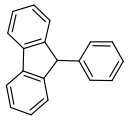
4[a]	310	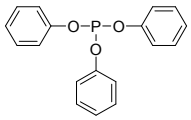
5	258	?
6	332	polyaromatic hydrocarbon
7	334	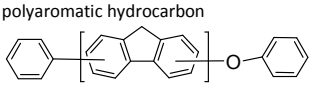

[a] *m/z*: 310, 217, 199, 170, 153, 112, 94, 77, 65, 51

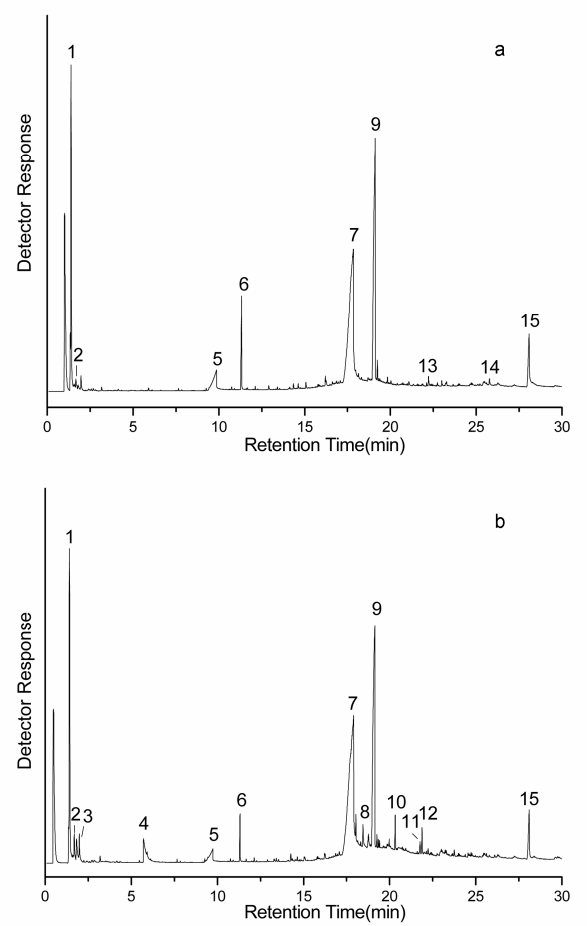

Fig. 7 Gas chromatogram of the gaseous pyrolysis products of PBT (a) and PBT/CPFP25% (b) obtained on heating at 600 °C (50 °C/min) for 1 min. For peak assignment see Table 4 (a) and Table 5 (b).

Table 4 The pyrolysis products of PBT at 600 °C

Peak No.	Molecular mass (*m/z*)	Compound
1	44, 54	CO_2 , $H_2C{=}CHCH{=}CH_2$
2	72	
5	122	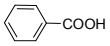
6	176	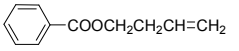
7	220	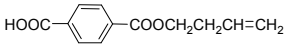
9	274	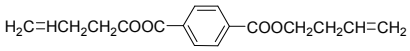
13	298	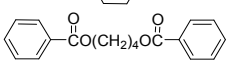
14	310	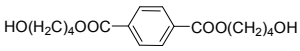
15	396	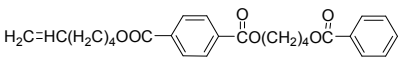

pyrolysis/GC/MS analysis. A typical chromatogram is shown in Fig. 6 and reports the formation of benzene, phenol, triphenyl phosphite and polyaromatic hydrocarbon. Neat PBT and PBT/CPFP25% was heated at 600 °C for 1 min. Fig. 7 shows the total ion gas chromatogram of the gaseous pyrolysis products.

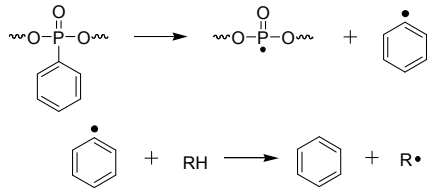

Fig. 8 Formation of benzene on the pyrolysis of PBT modified by CPFP.

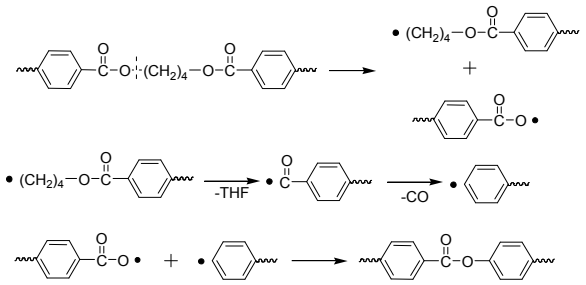

Fig. 9 Formation of polyarylates on the pyrolysis of PBT modified by CPFP.

Table 5 The pyrolysis products of PBT/CPFP25% at 600 °C

Peak No.	Molecular mass (*m/z*)	Compound
1	44, 54	CO_2 , $H_2C{=}CHCH{=}CH_2$
2	72	
3	78	
4	94	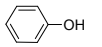
5	122	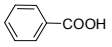
6	176	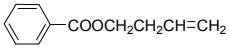
7	220	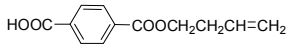
8	242	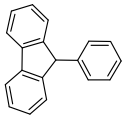
9	274	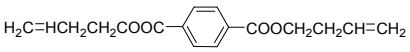
10	258	?
11	346	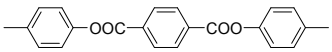
12	310	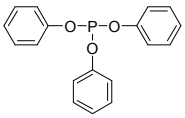
15	396	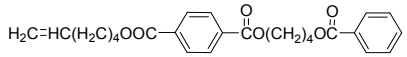

The assignment of the peaks is listed in Table 4 and Table 5. The main pyrolysis products of neat PBT are basically the same as that reported before.[27] The main pyrolysis products of PBT are 1,3-butadiene, terephthalic acid, and mono- and di-3-butenyl esters of terephthalic acid. New product evolves, benzene, phenol, which results from CPFP (Fig. 7). This implies a scission of the P-Ph bond, which is in agreement with the energy of the P-C bond is lower than that of the P-O-(C) bond. The formation of benzene on the pyrolysis of PBT modified by CPFP was shown in Fig. 8. According to McNeil and Bounekhel,[28] one of the homolysis routes results

from scission at the next alkyl oxygen bond as indicated in Fig. 9 (Fig. 7, product 11). In conclusion, the pyrolysis/GC/MS data support the thermogravimetric evidence that CPFP changed the degradation path of PBT as new products were formed.

Infrared study of residues

Fig. 10 shows the IR spectra of the initial CPFP (spectrum a) and of its solid residue obtained at 20% weight loss (b) and 520 °C (c). In the progress of heating from room temperature to 520°C, the sharp band at 1502 and 829 cm^{-1} (Spectrum a) associated with the para-substituted aromatic ring decreased in intensity, and a new band at 1407 cm^{-1} (Spectrum b) that might have aromatic character appeared. The 1600 cm^{-1} (the aromatic ring stretch) band persisted the heating, becoming broader. A formation of polyaromatic structures and the appearance of P-OH functionalities (broad absorption band between 1700 and 1600 cm^{-1}) are very likely the reasons for this.[29] The P-OH functionalities are supported by the development of the strong absorption band around 1006 and 530 cm^{-1}. The 1017 cm^{-1} band due to the P-O-C stretch persisted heating and became broad because of superimposition with the absorption bands at 1006 cm^{-1} (P-OH) and 931 cm^{-1} (P-O-P). The 691 cm^{-1} band related to mono-substituted aromatic rings decreased and the 1269 cm^{-1} band due to P=O stretch still persisted.

Most CPFP absorption bands are recognizable in the IR spectrum of the virgin formulation PBT/CPFP25% (Fig. 11, spectrum a).The bands are located at 1269, 1169, 1017 cm^{-1}. In addition, the spectrum shows bands due to (CH_2-CH_2) at 2921 and 2851 cm^{-1}, (C=O) at 1717 cm^{-1}, (O-CH_2) at 1102 cm^{-1} and (CH aromatic) at 729 cm^{-1} due to PBT.

As the weight loss increased to about 20% (Fig. 11, Spectrum b), new bands at 2661, 2541, 1692 and 1402 cm^{-1} being characteristic of aromatic carboxylic acid groups were formed.[22] New bands indicated the formation of anhydride groups (1795 and 1202 cm^{-1}) and vinyl groups (small band at 3077 cm^{-1}). The residue remaining after 50% weight loss (Fig. 11, Spectrum c) exhibits the broad absorption bands at 2200-2300 cm^{-1} due to P-OH stretch. Further heating to the main stage of weight loss (Fig. 11, Spectrum d), the bonded to the methylene group at 2921 and 2851 cm^{-1} and the

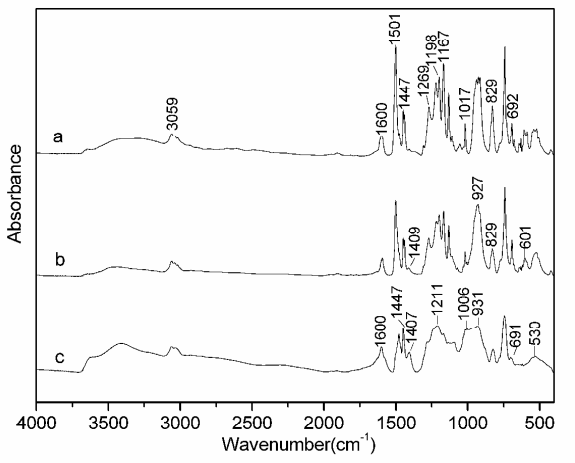

Fig. 10 Infrared spectra of initial CPFP (a) and its solid product of the thermal decomposition collected at 20% weight loss (b), 520 °C (c). KBr pellets.

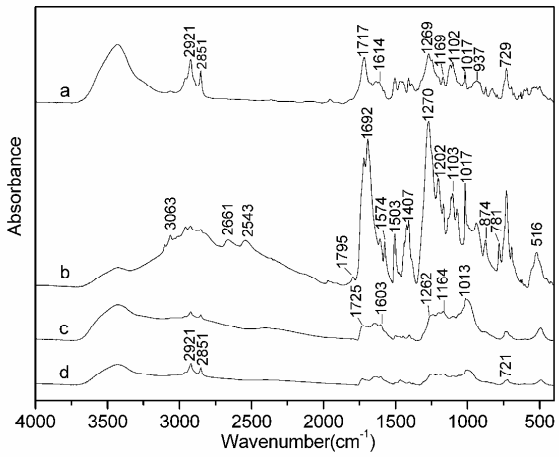

Fig. 11 Infrared spectra of initial PBT/CPFP25% (a) and solid products of the thermal decomposition of the mixture collected during thermogravimetry at different steps of weight loss in inert atmosphere: 20% weight loss (b), 50% weight loss (c), and after the main stage of weight loss (d). KBr pellets.

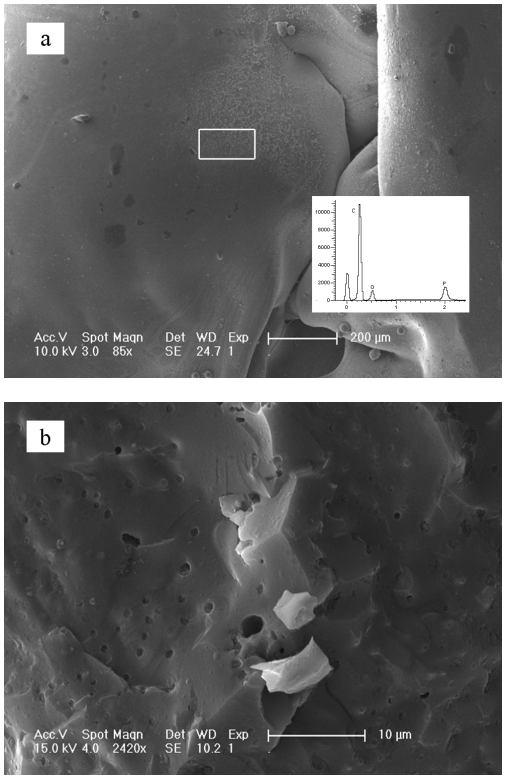

Fig. 12 SEM images of PBT/CPFP25% composite char: the outer surface (a), the inner surface (b).

aromatic C-H (720 cm^{-1}) are still detected in the solid residue. The 1269 and 1169 cm^{-1} bands due to P=O stretch and 1725 cm^{-1} due to C=O stretch in polyarylates still persisted.[28, 29] In conclusion, from the FTIR investigations reported above it becomes quite obvious that CPFP promotes the aromatization of PBT during thermal degradation which is thought to be caused by an active participation of CPFP in the chemical processes going on. The

addition of CPFP apparently changed the degradation pathways of PBT.

Morphology of residues

The PBT/CPFP25% composite was burnt during the UL-94 test, and its residue was collected for the test. From Fig. 12 (a) and (b), the PBT/CPFP25% outer char residue presented a compact and continual char layer that can provide a much better barrier to heat transfer and combustible gases and then interfere the combustion of the materials. Interior char residue with many small holes was formed by gaseous products in the process of burning. Stable and integrated char structures improve flame retardancy. Moreover, char structures cannot be destroyed even at high temperature, and the morphologies of residual chars can explain the efficient flame retardancy of CPFP. Thus, both thermal behavior and flammability properties were improved.

Energy-dispersive spectrometry (EDS) measurements suggested the enrichment of P, C, and O elements on the surface of PBT/CPFP25% char composite. EDS revealed that the residual chars contained polyphosphoric or phosphoric acid, which serves a function in the carbonization process. During burning, phosphorus in polymers is converted to phosphoric acid, and further thermal decomposition leads to the formation of polyphosphoric acid. Polyphosphoric acid simultaneously forming phosphorus-rich carbonaceous layer further inhibits the pyrolytic reactions. These dates were in agreement with the infrared study of residues.

Conclusions

A novel solid flame retardant cyclic 9,9-bis(4-hydroxyphenyl)fluorine (phenylene phosphonate) oligomer was synthesized in high yields by reaction of PPD with 9,9-bis(4-hydroxyphenyl)fluorine under pseudo-high-dilution conditions. The cyclic structure of the CPFP oligomer was confirmed by FTIR, ^{1}H NMR, ^{31}P NMR and MALDI-TOF-MS. CPFP oligomer was as flame retardants added to the PBT by melt blending. TGA showed that CPFP improved the residual char formations of composites but had no significant effect on the curve. Addition of CPFP apparently changed the pyrolysis pathways of PBT by formation of thermally stable polyarylates and phenolic groups. An increase of LOI was observed, and the UL-94 test V-0 rating was achieved by the addition of CPFP. PBT/CPFP blends can reach a V-0 rating of UL-94. Finally, SEM images showed that the residue with a continuous outer surface and porous internal structure provided a good barrier to improve the thermal behavior and flammability properties of the composites during burning.

In addition, the cyclic oligomer flame retardant may good at material compatibility and thermal stability and difficult to migrate. So that the cyclic oligomer flame retardant may have more broad application prospects.

Notes and references

1 Levchik SV and Weil ED, *Polym. Int.*, 2005, 54, 11-35.
2 Bernhard S, *Mater.*, 2010, 3, 4710-4745.
3 Levchik SV and WeilE D.A, *J. Fire. Sci.*, 2006,24, 345-364.
4 M. Despinasse and B. Schartel, *Polym. Degrad. Stab.*, 2012, 97, 2571-2580.
5 X. Wang, L. Song and W. Y. Xing, *Mater. Chem. Phys.*, 2011, 125, 536-541.
6 X. Wang, Y. Hu and L. Song, *Prog. Org. Coat.*, 2011, 71, 72-82.
7 X. Wang, Y. Hu and L. Song, *Anal. Appl. Pyrol.*, 2011, 92, 1641-1670.
8 H. Y. Ma, L.F. Tong and Z. B. Xu, *Polym. Degrad. Stab.*, 2007, 92, 720-726.
9 Chen DQ, Wang YZ and Hu XP, *Polym. Degrad. Stab.*, 2005, 88, 369-356.
10 Wang DY, Ge XG and Wang YZ, *Macromol. Mater. Eng.,* 2006, 29, 638-665.
11 D. Y. Wang, L. Wang and C. Wang, *Chengdu, China: CWYCC*, 2004.
12 Wang DY, Wang YZ and Wang JS, *Polym. Degrad. Stab.*, 2005, 87, 171-176.
13 Levchik GF, Grigoriev Yu V, Balabanovich AI, Levchik SV and Klatt M, *Polym. Int.,* 2000, 49, 1095-1100.
14 A. I. Balabanovich, A. M. Balabanovich and J. Engelmann, *Polym. Int.*, 2003, 52, 1309-1314.
15 A.I. Balabanovich, G. F. Levchik and S. V. Levchik, *J. Fire. Sci.,* 2002, 20, 71-83.
16 A.I. Balabanovich, *J. Anal. Appl. Pyrol.*, 2004, 72, 229-233.
17 E. A. Murashko, G. F. Levchik, S. V. Levchik, D. A. Bright and S. Dashevsky, *J. Appl. Polym. Sci.*, 1999, 71, 1863-1872.
18 Guo QZ and Chen TL, *Chem. J. Chinese. U.*, 2003, 24, 909-912.
19 Zhang HM, Guo QZ and Chen TL, *Chinese. J. Polym. Sci.*, 2004, 22, 83-89.
20 H. Jacobson and W.H. Stockmayer, *J. Chem. Phys.*, 1950, 18, 1600-1605.
21 Teasley MF, Wu DQ and Harlow RL, *Macromolecules*, 1998, 31, 2064-2074.
22 A. I. Balabanovich, T. A. Zevaco and W. Schnabel, *Macromol. Mater. Eng.*, 2004, 289, 181-190.
23 A.I. Balabanovich, *Polym. Degrad. Stab.*, 2007, 84, 451-458.
24 A.I. Balabanovich, G. F. Levchik and S. V. Levchik, *J. Fire. Sci.*, 2002, 20, 71-83.
25 A. I. Balabanovich, A. M. Balabanovich and J. Engelmann, *Polym. Int.*, 2003, 52, 1309-1314.
26 A. I. Balabanovich, *J. Fire. Sci.*, 2003, 21, 285-298.
27 J. F. Xiao, Y. Hu, L. Yang, Y.B. Cai, L. Song and Z. Y. Chen, *Polym. Degrad. Stab.*, 2006, 91, 2093-2100.
28 I. C. McNeill and M. Bounekhel, *Polym. Degrad. Stab.*, 1991, 34, 187-204.
29 L. Costa, M. Avataneo, P. Bracco and V. Brunella, *Polym. Degrad. Stab.,* 2002, 77, 503-510.